

Table 2. Concentration data for suspended particulate material in Arctic Ocean water at Arctic drifting ice station, T-3.

Water mass	Dry weight (mg/200 liters)	Position of sample from surface (m)	Water depth (m)	Latitude	Longitude
Surface	6.4	12	1537-1735	78°46'N	175°25'W
Pacific (maximum T)	3.76	75	2500-2528	79°25'N	171°25'W
Pacific (minimum T)	3.58	155	2286-2313	79°24'N	173°57'W
Atlantic	9.76	500	2184-2284	79°16'N	175°05'W
Deep water	1.16	1000	2498-2522	79°37'N	171°41'W
Deep water	1.92	2000	2250-2407	79°43'N	173°38'W
Deep water	1.68	2210	2310	79°39'N	171°52'W
Deep water	1.90	2260	2310	79°39'N	171°56'W
Deep water	2.0	2302	2304	79°38'N	172°00'W

liters) toward the continental slopes (6). At the continental slopes, "clouds" were observed with a larger content of particles in suspension, which are suggestive of nepheloid water.

Contamination, the addition of something foreign to the sample, is probably the greatest potential source of error. A concerted effort has been made for cleanliness in handling the water barrel, the pump and hoses to it, and the core pipe. Problems inherent to the sampling process prompted development of a recorder which gives a positive check on the depth of closing of the door of the barrel. The completeness of the recovery of the solids from the centrifugation process is checked by running the water remaining in the centrifuge bowl through Millipore filters. The amount of material that collects on these filters appears to be negligible.

Recent sampling with a 200-liter water barrel at the Arctic drifting ice station, T-3, provides a useful comparison with the shipboard sampling. At T-3, there is no core pipe, no storage tank, no pump or hoses to clean, and since the barrel used at T-3 has an air vent at the top and a spigot at the bottom, there is far less chance of contamination. Temperature and salinity define the stratification of four water masses (7) at the Arctic station, surface water, Pacific water, Atlantic water, and deep water. The concentrations of the particulate matter suspended in the Atlantic and Pacific water masses sampled at T-3 (Table 2) fall in the range of 0 to 9.9 mg/200 liters. The correlation of the T-3 value for Atlantic water, 9.76 mg/200 liters, with the mean value for the North Atlantic, 9.8 mg/200 liters is notable.

The mean values for clear ocean water indicate the South Pacific has the least amount of solids in suspension, the quantity increasing in the North

Pacific, then the North Atlantic, and is greatest in the South Atlantic. Certain areas of cloudy, or nepheloid, water have been shown, by photographically recording light scattering and by sample weight, to contain greater concentrations of sedimentary material in suspension than found in clear ocean water.

To this picture of sediment distribution in suspension, seismic profiles add the aspect of sediment stratification from the sea bottom to the crystalline basement rock. It appears that where a thick accumulation of pelagic sediments occurs, there is a nepheloid layer above, extending up from the sea bottom several hundred meters. Observations (8) indicate that oceanic deposition occurs in the nepheloid layer. The relationship is significant because it is part of the sedimentation process which may have been active for hundreds of millions of years. Areas receiving vast accumulations of sediments today, such as the North American Basin or the Argentine Basin, may have continued to do so throughout one and perhaps part of two geologic eras.

The pelagic sediments found in these basins have many origins, terrigenous, volcanic, extraterrestrial, skeletal, or chemical precipitation; fine grain-size, however, is their prevailing character-

istic. Material of less than one micron in size, especially clay minerals, is found in even the clearest water of the mid-ocean. Because of their size and shape, clay mineral flakes can be carried in suspension for long periods of time by currents and circulation of the deep sea. Similarly lutite-size material half-settled and half-suspended at the sediment-water interface may be disturbed, resuspended, and reactivated into a lutite flow, a fine-grained analog of a turbidity flow. Such a process could explain the distribution of pelagic sediments. The flow would follow the bottom topography, transported by the movement of bottom water, and produce deposits of colloidal-size particles that would blanket and eventually smooth out basement irregularities (9) exactly as seismic profiles portray pelagic stratification.

MARIAN B. JACOBS
MAURICE EWING

Lamont Geological Observatory,
Columbia University, Palisades,
New York 10964

References and Notes

1. M. Ewing and E. M. Thorndike, *Science* **147**, 1291 (1965).
2. M. Ewing, S. L. Etreim, J. I. Ewing, X. Le Pichon, in *Physics and Chemistry of the Earth* (Pergamon, New York, in press).
3. D. W. Folger and B. C. Heezen, *Abstr. Geol. Soc. Am.*, NE Section (1967).
4. S. Eitrem, personal communication (1968).
5. B. Kullenberg, *Tellus* **5**, 302 (1953).
6. A. P. Lisitzin, *Oceanogr. Res.* **2**, 71 (1960).
7. L. V. Worthington, "Scientific studies at Fletcher's Ice Island, T-3, (1952-1955)," *Geophys. Res. Paper 63* (Air Force Cambridge Research Center, Bedford, Mass., 1959), vol. 1, p. 31.
8. M. Ewing, *Quart. J. Roy. Astron. Soc.* **6**, 10 (1965).
9. M. Ewing, W. J. Ludwig, J. I. Ewing, *J. Geophys. Res.* **69**, 2003 (1964); M. Ewing and J. Ewing, *An. Acad. Brasil. Cienc.* **37**, 31 (1965).
10. Supported by NSF GA 419 and GA 959. We thank D. Rowland for laboratory assistance, T. Aitken, J. Goddard, J. Cromwell, Dr. J. Hays, and others for shipboard work. At T-3, G. Mathieu collected the samples and concentrated them under ONR contract Nonr 266 (82) and support from the Vetlesen Foundation. We thank Drs. K. Hunkins and J. Hays for suggestions. Lamont Geological Observatory (Columbia University) contribution No. 1286.

13 August 1968; revised 22 November 1968 ■

Fossil Deep-Sea Channel on the Aleutian Abyssal Plain

Abstract. *The discovery of a leveed deep-sea channel whose axial gradient reverses near the Aleutian trench supports the hypothesis that the downbowing of the trench interrupted the turbidity current processes that constructed the Aleutian abyssal plain.*

A study of fathograms (1) from Environmental Science Services Administration Seemap surveys has revealed a deep-sea channel which trends northeast to southwest for a distance of 370 km

on the Aleutian abyssal plain south of the Aleutian trench (Fig. 1). The channel, here named Seemap channel, is unusual in that it slopes downward from a summit located about midway from

either end (Fig. 2a), thus precluding the flow of turbidity currents from end to end. It is postulated that the section northeast of the present summit was once higher, but has been downwarped with the Aleutian trench, thus cutting the channel off from a northern source. This is in agreement with the thesis suggested by Hurley (2) from bathymetric considerations and supported by Hamil-

ton's (3) seismic reflection results that the Aleutian plain has been cut off from its supply of turbidites by the Aleutian trench, leaving a fossil or relic abyssal plain whose only present-day supply of sediment is pelagic material settling from the water column.

The profiles across the channel shown in Fig. 2b are typical of the channel northeast of point *B* (Fig. 1). Its width,

measured between the highest parts of the levees, averages about 6 km, and its depth (top of levees to channel bottom) averages about 50 m. West of *B*, the channel loses its distinctive shape as it turns into a region of east-west trending ridges. Farther west it widens and becomes indiscernible as a single feature. Upstream from point *E* (Fig. 1), the channel passes close to Sirius Seamount

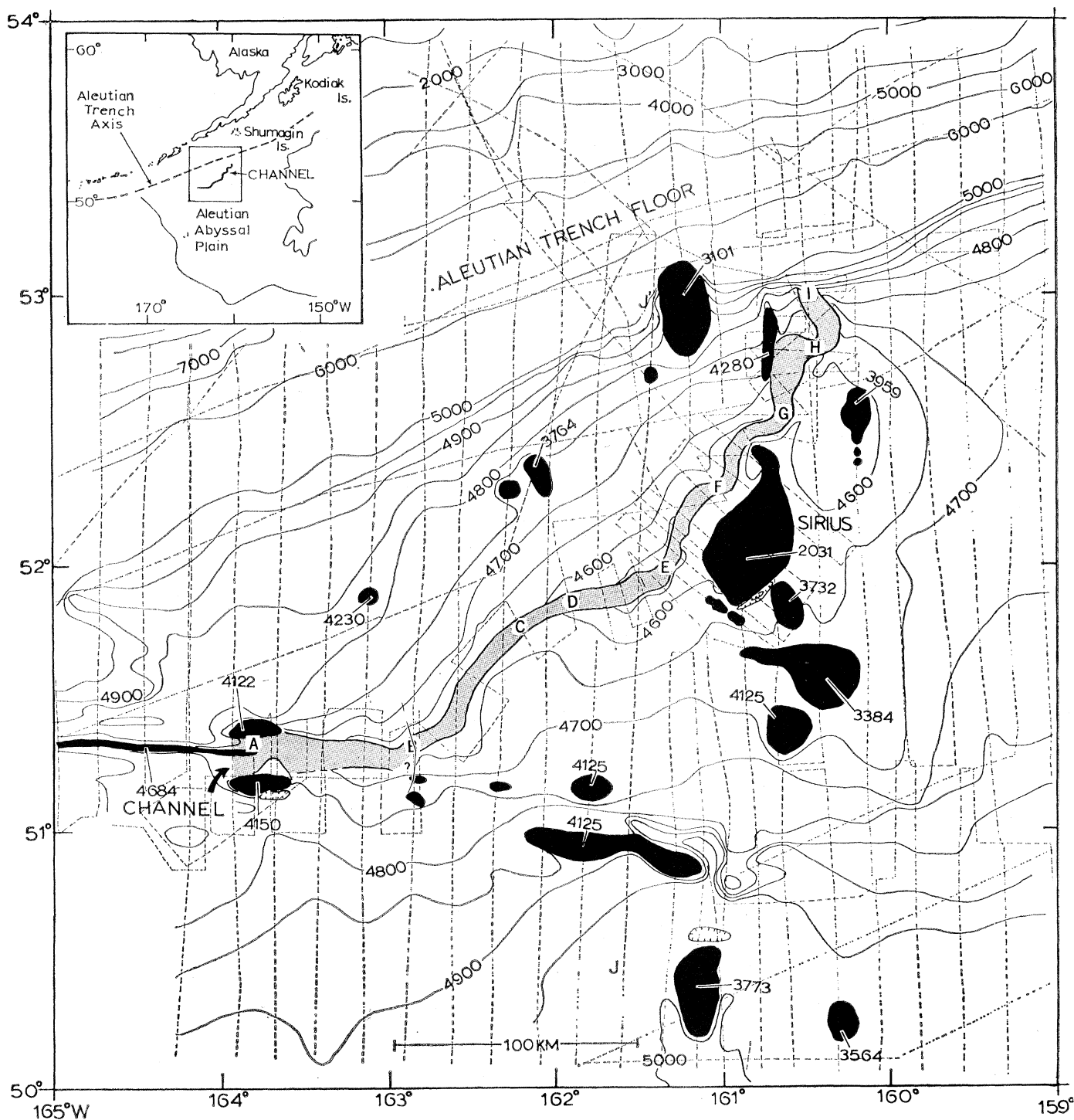


Fig. 1. Location of Seamap channel on the Aleutian abyssal plain. The channel is shaded between the highest parts of the levees. Depths are in corrected meters. Seamounts, ridges, and abyssal hills are shown in black. Tracklines are dashed. The contour interval changes north of the 5000-m contour on the south wall of the Aleutian trench. Letters *A* to *I* correspond to points along the axial profile shown in Fig. 2.

and has well-developed meanders averaging about 35 km in wavelength. It finally disappears at a depth of about 4800 m on the south wall of the Aleutian trench (Fig. 1, *D*); north of point *I* it has apparently been destroyed by slumping.

The direction that turbidity currents flowed when the channel was active must have been from northeast to southwest because (i) the only plentiful supply of material for turbidites is continental North America which is northeast of the channel; (ii) in general the Aleutian abyssal plain deepens toward the south; and (iii) to the southwest of point *E* (Fig. 1), where the relative heights of the channel levees have apparently been little affected by the formation of the trench (and where the channel does not meander), the right levee (as one looks southwest) is consistently higher than the left levee. This is consistent with observations that in the northern hemisphere, as one looks downstream, the levee on the right side is higher as a result of the Coriolis effect (3, 4).

It is difficult to tell how closely the axial profile (Fig. 2a) approximates the profile which existed immediately after the trench formed, and which parts of it, if any, represent the channel before the trench formed. The section of profile from *A* to *E* may be close to that of the channel when it was active. The minor gradient reversals in this section of the channel could be the results of processes, operating during or after the trench formed, such as regional warping of the sea floor or nonuniform pelagic sedimentation rates.

The downbowed part of the profile (between *E* and *I*, Fig. 2a) shows three secondary peaks. These possibly are caused by the greater downbowing by the Aleutian trench of the north swings of the meanders impressed on an irregular original gradient.

The trend of Seemap channel is along the crest of a broad rise, with the floor of the channel elevated well above the general level of the adjacent area (Fig. 1 and Fig. 2c). Similar but less pronounced channel elevations have been observed elsewhere in the northeast Pacific (3). Hamilton's seismic reflection data for channels in the northeast Pacific clearly show that deep-sea channels are depositional features (3). This suggests that Seemap channel is located on an unusually thick wedge of sediment.

Assuming that the axial gradient

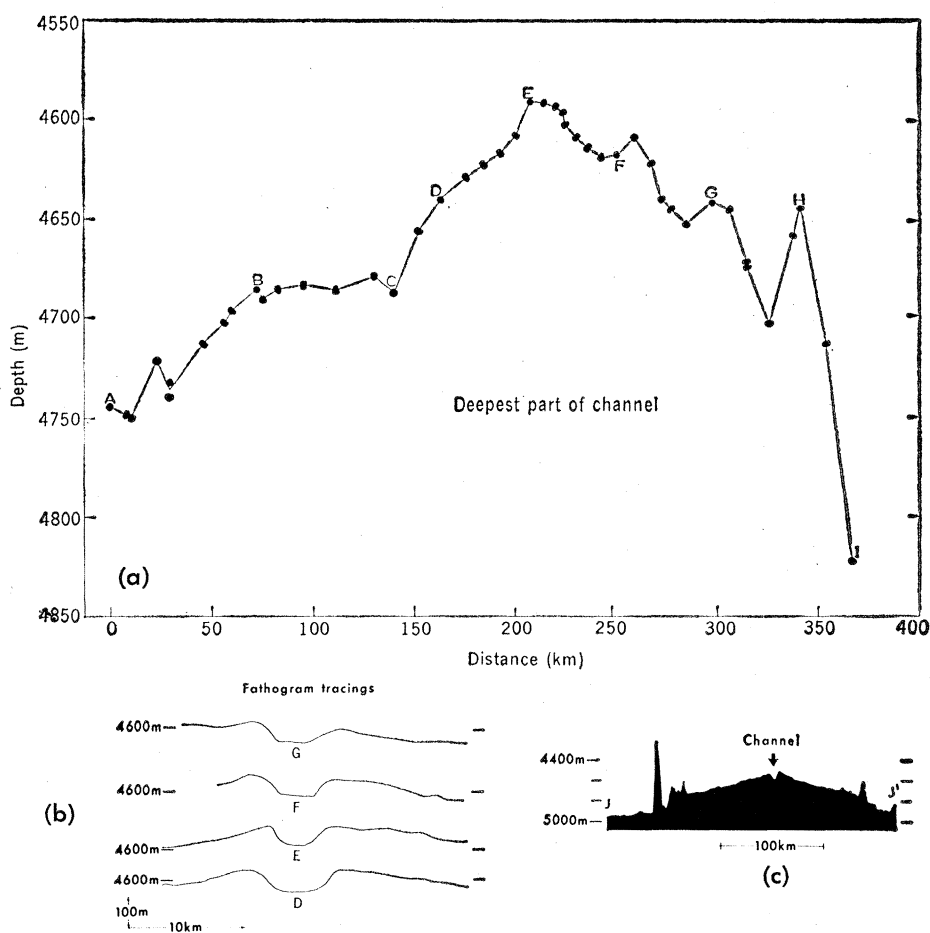


Fig. 2. (a) Longitudinal (axial) profile of Seemap channel. Vertical exaggeration is 1000. Letters *A* to *I* are points along the channel shown in Fig. 1. (b) Profiles across channel from echo soundings at points *D*, *E*, *F*, and *G* looking southwest. Vertical exaggeration about 30. (c) North-south profile across region along section *J*-*J'* of Fig. 1 (vertical exaggeration of 100).

which existed before the trench formed is approximated by that portion of the channel southwest of point *E*, we can compare its gradient with that of other active channels. The mean gradient from *A* to *E* is 0.75 m/km. However, it shows much variability (it is essentially zero between *B* and *C*, and 1.4 m/km between *C* and *E*). Cascadia channel, which has an axial profile similar to those of other channels, has gradients of 1.83, 1.67, and 1.17 m/km at respective distances of about 165, 275, and 435 km from the base of the continental slope (2). Although there are many difficulties in using such comparisons to obtain an approximate distance of section *A* to *E* from the ancient source of turbidites, it seems reasonable that this part of the channel was at least several hundred kilometers from the sediment source. An extrapolation of the channel north of the trench suggests that it may have originated somewhere in the area between the Shumagin Islands and Kodiak Island. However, our

echo soundings (mainly along north-south lines) have not revealed the presence of the channel north of the trench.

PAUL J. GRIM
FREDERIC P. NAUGLER
*Pacific Oceanographic Research
Laboratory, Seattle, Washington 98102*

References and Notes

1. The channel was first revealed by an examination of echo soundings taken by the U.S. Coast and Geodetic Survey ship *Pioneer* from 1961 to 1963. During April 1968, a 3-day study of the channel was conducted from the *Oceanographer* with the use of satellite-controlled navigation. Six additional crossings of the western part of the channel were made by the ship *Surveyor* in June 1968. All records were read to the closest fathom (1.83 m) and converted to corrected meters according to the method described by T. V. Ryan and P. J. Grim [*Int. Hydrograph. Rev.* 45, 41 (1968)].
2. R. J. Hurlley, *Scriptas Inst. Oceanogr. Ref.* 60-7 (1960), p. 1.
3. E. L. Hamilton, *J. Geophys. Res.* 72, 4189 (1967).
4. H. W. Menard, Jr., *Bull. Amer. Ass. Petrol. Geol.* 39, 236 (1955); H. W. Menard, S. M. Smith, R. M. Pratt, in *Submarine Geology and Geophysics*, W. F. Whitford and R. Bradshaw, Eds. (Butterworths, London, 1965), p. 271. A more detailed description of the channel and a discussion of differences in levee heights and their causes is in preparation.

5. We thank C. A. Burk, B. H. Erickson, E. L. Hamilton, R. J. Hurley, T. V. Ryan, and H. B. Stewart, Jr., for discussions about the channel. The navigational skill of the officers and crew of the *Pioneer, Surveyor*, and *Oceanographer* made this study possible.

13 September 1968; revised 22 November 1968

Garnet-Like Structures of High-Pressure Cadmium Germanate and Calcium Germanate

Abstract. Crystals of CdGeO_3 grown at a pressure of 65 kilobars are tetragonal and have an ordered, garnet-like crystal structure with cadmium occupying the dodecahedral and octahedral sites, and germanium the octahedral and tetrahedral sites. The crystal structure ($a = 12.406 \pm 1$ angstroms, $c = 12.256 \pm 1$ angstroms, and space group $I4_1/a$) has been refined by least-squares analysis to an R (discrepancy index) of 0.073. Two high-pressure phases of CaGeO_3 were synthesized, one isotypic with tetragonal CdGeO_3 ($a = 12.514 \pm 3$ angstroms, $c = 12.358 \pm 3$ angstroms), and the other isotypic with perovskite.

In 1963 Ringwood and Seabrook (1) reported the synthesis of a high-pressure phase of CaGeO_3 which apparently had the garnet structure. They also synthesized CdGeO_3 , which had an x-ray powder pattern similar to that of garnet except that the reflections were split; this indicated that the symmetry was lower than cubic. Ringwood and Seabrook proposed the formula $\text{Cd}_3^{\text{VIII}}(\text{CdGe})^{\text{VI}}\text{Ge}_3^{\text{IV}}\text{O}_{12}$. However, CaGeO_3 also has the lower symmetry, and its x-ray powder patterns can be indexed on a tetragonal cell with $a = 12.51 \text{ \AA}$,

$c = 12.36 \text{ \AA}$ (2). Because there has been considerable comment about anisotropic optical properties of garnet (3) and because, to our knowledge, no other modifications of garnet with symmetry lower than cubic have been reported, we have investigated the high-pressure CdGeO_3 and CaGeO_3 phases to determine the actual symmetry and have refined the crystal structure of CdGeO_3 because we could prepare better crystals of this phase.

High-purity CdO and GeO_2 in a 1:1 molar ratio were thoroughly mixed. The mixture was subjected to a pressure of 65 kb at 1200° to 1400°C for about 4 hours and then quenched. Two CaGeO_3 phases were prepared by analogous high-pressure methods, except that the starting material was CaGeO_3 with the wollastonite structure. One of these phases has the garnet-like structure (1, 2), and the other is isotypic with perovskite. The tetrahedral anvil used for these high-pressure experiments has been described by Bither *et al.* (4).

A Hagg-Guinier photograph was initially taken of the CdGeO_3 sample. We assumed that the cell was tetragonal with $a \sim c \sim 12.40 \text{ \AA}$; using a computer program for the assignment of indices and refining by least-squares analysis, we were able to index the pattern and to refine the cell. These results were confirmed with precession photographs of a single crystal, and the space group was identified as $I4_1/a-C_{4h}^{16}$ [absences: for hkl , $h+k+l \neq 2n$ and for $hk0$, $h(k) \neq 2n$]. Other cell data are $a = 12.406 \pm 1 \text{ \AA}$, $c = 12.256 \pm 1 \text{ \AA}$, cell volume (V) = $1.886.3 \text{ \AA}^3$, number of formula units per cell (Z) = 32, calculated density (D_p) = 6.56 gm^{-3} , and absorption coefficient $\mu = 115.0 \text{ cm}^{-1}$

($\text{AgK}\alpha$ radiation). The cell for tetragonal CaGeO_3 has $a = 12.514 \pm 3 \text{ \AA}$, $c = 12.358 \pm 3 \text{ \AA}$; we have assumed that CaGeO_3 has the same space group as CdGeO_3 , although no crystals large enough for single-crystal examination have been synthesized. The observed and calculated powder patterns for CdGeO_3 and CaGeO_3 have been submitted to the powder data file of the American Society for Testing and Materials.

Ringwood and Major (5) reported the synthesis of a perovskite form of CaGeO_3 at 120 kb and 900°C . This compound appeared to be cubic with $a = 3.723 \text{ \AA}$. Although one of the phases in our samples of CaGeO_3 is also the perovskite type, it would be necessary to double the cell parameter ($7.448 \pm 2 \text{ \AA}$) to account for weak reflections on both the Guinier and precession photographs.

Using a Picker diffractometer with Pd-filtered $\text{AgK}\alpha$ radiation, a takeoff angle of 3° , pulse-height analysis, and a scan range for each reflection of 1.5° plus the ($\alpha_1 - \alpha_2$) dispersion, we measured three-dimensional diffraction data (740 nonequivalent reflections). These data were corrected for absorption, and provision was later made for secondary extinction correction during least-squares refinement.

We devised a model for the structure by comparing possible locations in space group $I4_1/a$ with those of the garnet structure in $Ia3d$. In doing this, it was necessary to shift the origin of $I4_1/a$ by $\frac{1}{2}, \frac{1}{4}, \frac{1}{8}$ from that given in *International Tables for X-Ray Crystallography* (origin at $\bar{4}$) (6). This orients the symmetry elements of $I4_1/a$ in a manner similar to those for $Ia3d$ (6). Table 1

Table 1. Relations between equivalent positions in the garnet and CdGeO_3 structures and the refined CdGeO_3 atom coordinates and isotropic temperature factors.

Garnet space group $Ia3d$				CdGeO ₃ space group $I4_1/a$						
Site	Equi-point	Symmetry	Coordinates	Atom	Equi-point	Symmetry	Refined coordinates			B (Å ²)
							x	y	z	
Dodecahedral	24c	222	$\frac{1}{2}, 0, \frac{1}{4}$	Cd(1)	16f	1	0.1256 ± 1	0.0052 ± 1	0.2564 ± 1	0.64 ± 5
				Cd(2)	8e	2	0	$\frac{1}{4}$	$.6236 \pm 2$	$.61 \pm 6$
Octahedral	16a	$\bar{3}$	0,0,0	Cd(3)	8d	$\bar{1}$	0	0	$\frac{1}{2}$	$.63 \pm 6$
				Ge(1)	8c	$\bar{1}$	0	0	0	$.43 \pm 7$
Tetrahedral	24d	$\bar{4}$	$\frac{1}{8}, 0, \frac{3}{8}$	Ge(2)	4b	$\bar{4}$	0	$\frac{1}{4}$	$\frac{3}{8}$	$.50 \pm 9$
				Ge(3)	4a	$\bar{4}$	0	$\frac{1}{4}$	$\frac{7}{8}$	$.36 \pm 9$
				Ge(4)	16f	1	$.1267 \pm 2$	$.0166 \pm 2$	$.7599 \pm 2$	$.37 \pm 6$
				O(1)	16f	1	$.0251 \pm 11$	$.0672 \pm 11$	$.6718 \pm 12$	$.41 \pm 27$
Oxygen	96h	1	x,y,z	O(2)	16f	1	$.0478 \pm 11$	$.0500 \pm 11$	$.8621 \pm 11$	$.36 \pm 28$
				O(3)	16f	1	$.2260 \pm 11$	$.1117 \pm 12$	$.8101 \pm 11$	$.41 \pm 27$
				O(4)	16f	1	$.2148 \pm 11$	$-.0823 \pm 11$	$.7023 \pm 12$	$.28 \pm 26$
				O(5)	16f	1	$-.0653 \pm 11$	$.1636 \pm 12$	$.4696 \pm 12$	$.63 \pm 28$
				O(6)	16f	1	$-.1051 \pm 11$	$.2128 \pm 12$	$.7840 \pm 12$	$.59 \pm 28$